

# Strain mediated suppression of the metal-insulator transition in $\text{EuNiO}_3$ thin films

D. Meyers<sup>1</sup>, S. Middey<sup>1</sup>, M. Kareev<sup>1</sup>, M. van Veenendaal<sup>2</sup>, E. J. Moon<sup>1</sup>, B. A. Gray<sup>1</sup>, J. W. Freeland<sup>3</sup>, and J. Chakhalian<sup>1</sup>

*Department of Physics, University of Arkansas, Fayetteville, AR 72701*

*Dept. of Physics, Northern Illinois University, De Kalb, Illinois 60115, USA and*

*Advanced Photon Source, Argonne National Laboratory, Argonne, IL 60439, USA*

Ultrathin epitaxial films of  $\text{EuNiO}_3$  were grown on a series of substrates traversing highly compressive (-2.4%) to highly tensile (2.5%) lattice mismatch. X-ray diffraction measurements showed the expected c-lattice parameter shift for compressive strain, but no detectable shift for tensile strained substrates, while reciprocal space mapping confirmed the tensile strained film maintained epitaxial coherence. Transport measurements showed a successively (from tensile to compressive) lower resistance and a complete suppression of the metal-insulator transition at highly compressive lattice mismatch. Corroborating these findings, X-ray absorption spectroscopy measurements revealed a strong multiplet splitting in the tensile samples that progressively weakens with increasing compressive strain that, combined with cluster calculations, showed enhanced covalence between Ni-d and O-p orbitals leads to the metallic state.

## I. INTRODUCTION

Complex transition metal oxides are at the forefront of current research towards the understanding of the fundamental physics underlying several astonishing physical properties including high temperature superconductivity, colossal magnetoresistance, multiferroicity, and the thermally induced metal-insulator transition (MIT)[1–6]. In particular, the temperature driven MIT in correlated oxides has garnered remarkable investigation over last several decades. Understanding of the MIT and its control by external means such as pressure, magnetic field, confinement, and chemical doping is not only interesting from the physics point of view[7–10], but they also show great potential as candidates for future electronic devices[11]. Recent advances in material synthesis by utilizing the lattice mismatch between the substrate and the as-grown films have opened a new dimension in controlling and engineering the materials properties. This epitaxial strain leads to a restructuring of the grown material and an entirely coherently strained crystal can be obtained in the ultra thin limit. The effect of this lattice modulation on the materials properties can be quite dramatic[12–25] and is of particular interest as technology continues to accelerate towards the need for ultrathin film materials for electronic applications, and, thus, the need for a fundamental understanding of these effects is paramount.

The rare-earth (RE) nickelates  $\text{ReNiO}_3$  (Re = Pr, Nd, Eu, ...) in their bulk form, with Ni having formal +3 oxidation state ( $t_{2g}^6 e_g^1$ ), all display a metal-insulator transition, except Re = La, while the nature of the transition and its temperature ( $T_{MIT}$ ) depends strongly on the choice of Re cation as shown in Fig. 1[26–28]. The very distorted  $\text{ReNiO}_3$  with Re = Lu, Y, Eu, Sm, *etc.* first show a second order MIT at higher temperature while the spins remain in their paramagnetic state across the transition. These compounds further undergo another second order transition to a  $E'$  - type antiferromagnetic, insulating state at lower T ( $T_N$ ) along with possibly forming a charge ordered state, which is still controversial and not fully understood[29–33]. On the other hand, the members with intermediate distortion (*e.g.* Nd, Pr,  $\text{Sm}_{0.5}\text{Nd}_{0.5}$ ) exhibit a first order phase transition, accompanied by a small volume expansion,

directly from the paramagnetic metallic state to the  $E'$  - type antiferromagnetic insulating state, bypassing entirely the paramagnetic insulating region[27, 34–36]. Several technological applications have already been proposed and devices fabricated utilizing thin films of these materials [37–40]. From a technological point of view, control of the MIT is of great importance, however using different RE ions depending on application is impractical, as synthesis conditions and thermal stability can vary among them[12, 41–44]. Alternatively, it would be more practical, as well as more scientifically approachable, to use this obligatory strain in thin films as an avenue to engineer the physical properties within a particular RE nickelate as it can modulate the MIT and AFM transition significantly as observed for  $\text{NdNiO}_3$  [12, 13]. However, several key questions still need to be answered. Key among them, what effect will strain (tensile and compressive) have upon the phase diagram in Fig. 1 for the materials showing second order transitions? It has been shown, through powder studies, that external pressure suppresses the MIT while actually slightly raising the AFM transition, eventually leading to a surprising AFM, metallic state[45–47]. It is also possible that epitaxial strain can be used to take one of the more distorted nickelates, showing two second order transitions, and induce a first order phase transition via strain mimicking the results of chemical doping[48].

In this letter, we characterize several ultra thin epitaxially strained  $\text{EuNiO}_3$  (ENO) films grown on various substrates spanning both compressive and tensile strain using x-ray diffraction (XRD), reciprocal space mapping (RSM), electronic transport, and x-ray absorption spectroscopy (XAS) to elucidate the effects of epitaxial strain on the structural, electronic, and magnetic properties. The results of these methods display the capacity of epitaxial strain to modulate the physical properties of this highly distorted nickelate system. In addition, cluster calculations on a  $\text{NiO}_6$  octahedra allowed the extraction of the charge-transfer (CT) energy on the various films, shedding light on the source of the observed modulation in material's properties.

## II. EXPERIMENTAL

ENO films were grown on a variety of substrates incorporating lattice mismatches ranging from 2.5% to -2.4% using pulsed laser interval deposition, the details of which can be found elsewhere[44]. The substrates used for growth presented here are as follows:  $\text{YAlO}_3$  (YAO; -2.4% lattice mismatch),  $\text{SrLaAlO}_4$  (SLAO; -1.3%),  $\text{LaAlO}_3$  (LAO; -0.3%),  $\text{NdGaO}_3$  (NGO; 1.5%), and  $\text{LaGaO}_3$  (LGO; 2.5%). XRD measurements, besides ENO on YAO which is described elsewhere[44], were taken with a Panalytical X'Pert Pro MRD (Panalytical, Almelo, The Netherlands), equipped with a parabolic mirror and triple bounce / axis monochromator on the incident and diffracted beams, around the (002) (psuedocubic notation) truncation rod of the substrate. The same instrument was used to measure a RSM around the (-103) truncation rod. Transport properties were measured with a Quantum Design Physical Property Measurement System (PPMS) using a four point probe with the *Van Der Pauw* geometry. XAS measurements were taken at the 4-ID-C beam line of the Advanced Photon source at Argonne National Labs in total electron yield (TEY) mode on the Ni  $L_{2,3}$ -edges at 250° K.

Calculations were done for a  $\text{NiO}_6$  cluster with octahedral coordination using the methods described here[49]. The Hamiltonian includes the on-site Coulomb interaction between the 3d electrons and between the 3d electrons and the 2p core hole. The parameters are calculated within the Hartree-Fock limit and scaled down to 80% to account for intra-atomic screening effects. The monopole parts were  $F_{dd}^0 = 6$  and  $F_{pd}^0 = 7$  eV. The spin-orbit coupling was included for the 3d and 2p electrons. The hybridization with the ligands was taken into account by including configurations up to double ligand hole. The hybridization parameter is  $V = 2.25$ ; -1.03 eV for the  $e_g$  and  $t_{2g}$  orbitals, respectively. The cubic crystal field of 10 Dq is 1.5 eV.

## III. RESULTS

Fig. 2(a) shows  $2\theta - \omega$  scans around the (002) truncation rod for the 15 unit cell (uc) ENO films grown on different substrates ((006) rod for SLAO, due to its tetragonal structure). All films show a broadened film peak, due to the 15 uc thickness of the films, and a sharp substrate peak which was used to align each data set. The film peaks for the highly compressive films (YAO, SLAO) show a noticeable shift from the ENO lattice constant (represented by a dashed line) towards smaller  $2\theta$ , while for LAO no shift is observable. Films under tensile strain (NGO, LGO) show a well resolved film peak with no shift from the bulk value. Fig. 2(b) shows a RSM around the (-103) Bragg peak for a 35 uc ENO on NGO film. The weak film peak shares the same value for H (reciprocal lattice units) and a larger value for L.

DC transport was measured on the 15 uc films, shown in Fig. 3(a). The data was recorded during both cooling and heating cycles from 380 K to 2K, though no hysteresis was found and only warming curves are shown. For the tensile

cases the resistivity follows the expected bulk-like insulating behavior below 380K. For the small compressive strain case, LAO, the resistivity at lower temperatures separates from bulk behavior  $\sim 250$ K and begins increasing at a lesser rate. For the compressively strained SLAO the sample shows metallic behavior at high temperatures with a MIT occurring at 335K. The film on YAO is metallic down to 2K. Fig. 3(b) shows  $\frac{d \ln \rho}{d(\frac{1}{T})}$  vs T for all films besides ENO on YAO, with each showing a characteristic kink indicative of an AFM transition around 200K. Fig. 3(c) shows the extracted T values for the kinks, denoted  $T^*$ .

XAS measurements were taken on the Ni  $L_{3,2}$  - edges, plotted in Fig. 4(a). All films show a strong white line at  $\sim 855$  eV ( $\sim 872$  eV). Additionally, a shoulder around 853 eV (871 eV) is apparent for all films, being much larger for the tensile case and gradually decreasing as compressive strain is increased. A small peak around  $\sim 851$  eV corresponding to the La  $M_4$  edge appears for the substrates containing La. The size of the energy separation between the  $L_3$  and multiplet peak for each strain is shown in Fig. 4(b) in the left axis. The splitting decreases from the tensile strained films,  $\sim 1.8$  eV, with increasing compressive strain to  $\sim 1.2$  eV for YAO. Fig. 4(b) also shows the calculated CT energy (right axis) which follows a very similar trend.

## IV. DISCUSSION

Epitaxial strain is possible with these materials due to the extraordinary ability of the perovskite lattice to accommodate the strain through lattice and symmetry effects; it is these effects that ultimately lead to the observed modulation of the physical properties. Thus XRD is a very important technique to deduce how the lattice incorporates the strain and to check for secondary phase formation.  $2\theta$  values, corresponding to the film peaks in Fig. 2(a), were used to calculate the out-of-plane lattice constants. This yielded the following c-axis lattice parameters: 3.878 Å (YAO), 3.84 Å (SLAO), 3.80 Å (NGO), and 3.81 Å (LGO), while for LAO strong overlap between the strong substrate peak and film peak due to the small strain value, -0.5%, prevent a reliable c-axis lattice constant from being extracted and the weakness of the film peak is probably due to the severe twinning present on the LAO substrates. While for the samples with in-plane compressive strain the shift of the out-of-plane lattice constants from the bulk value of 3.80 Å is expected and consistent, the tensile strained substrates show no significant shift (0.26% for ENO on LGO, much lower than the 2.5% biaxial in-plane strain).

In order to ascertain whether or not this lack of c-axis lattice modulation was due to strain relaxation, unlikely in such thin films, a RSM was taken for a 35uc ENO film grown on NGO, Fig. 2(b). The thicker sample was needed in order to obtain a strong enough (-103) film peak with this in-house MRD system, and, being thicker than 15 uc, was *more* likely to show relaxation. The RSM around the (-103) reflection of the substrate shows a strong substrate peak with a broadened film peak at higher L (shown in reciprocal lattice units (r.l.u.)). The H value of this film peak matches well with that of the sub-

strate (demonstrated by the dotted line) confirming the film is coherent to the substrate, while the center  $L$  value of  $\sim 3.053$  r.l.u. gives an out-of-plane lattice constant of  $3.793 \text{ \AA}$ , in good agreement with the rocking curve measurement. This, along with the bulk-like  $c$ -axis lattice constant, implies the strain is compensated for by some other means, possibly as was found for  $\text{LaNiO}_3$  films under tensile strain[50]. In that case the occurrence of "breathing" modes were found that compensated for the  $a$ - $b$  lattice mismatch without affecting the  $c$ -axis lattice constant. X-ray linear dichroism (XLD) measurements and density functional theory calculations will be done in the future to confirm this.

Tracking the evolution of the MIT with lattice modulation in these epitaxially strained films revealed a very significant effect. As compressive strain is increased  $T_{MIT}$  is suppressed until entirely disappearing for the case of ENO on YAO (seen only for  $\text{Re} = \text{La}$  in bulk), highlighting the ability of utilizing lattice mismatch to engineer the behavior of physical phenomena. This sample was found to have linear  $T$  dependence above 200K, which is common to the  $\text{ReNiO}_3$  compounds in their metallic phase excluding  $\text{Re} = \text{La}$ , followed by  $T^{3/2}$  dependence below. The  $T^{3/2}$  dependence at low  $T$  was shown to be caused by enhanced scattering due to bond-length fluctuations, indicating strong electronic correlations and enhanced vibronic fluctuations of the charge ordered state, likely due to quantum confinement in these ultra thin films[51, 52]. In the case of SLAO, with intermediate compressive strain, linear  $T$ -dependent metallic behavior is followed by a MIT shifted to 335K, putting it enticingly close to room temperature which makes it a potential candidate for electronics applications. Interestingly, the tensile strained samples have nearly identical resistivities for all temperatures observed despite their considerably disparate strain values, possibly associated with the lack of  $c$ -axis deformation as observed with XRD. Unfortunately, the high temperature of the bulk MIT (480 K) prevents us from investigating the change in the  $T_{MIT}$  for LAO, NGO, and LGO films. With the lack of hysteresis, characteristic of first order phase transitions, our results suggest epitaxial strain does not induce a first order transition in this material, as was seen with chemical doping[36]. Instead they show compressive strain works to lower the transition temperatures as was seen with external pressure[35, 46, 47]. This is also strongly reminiscent of work on ultra thin films of  $\text{NdNiO}_3$ , where it was proposed that a closing of the CT gap was responsible for the quenching of the MIT with strain, analogous to changing the  $\text{Re}$  ion in bulk[12, 27]. To further investigate the possibility of epitaxial strain mimicking external pressure the AFM transition temperature,  $T_N$ , is needed..

In an attempt to locate the AFM transition temperature,  $\frac{d \ln \rho}{d(\frac{1}{T})}$  was investigated for all insulating samples, shown in Fig. 3(b). This analysis helps reveal the temperature where spin ordering occurs, and appears as a small kink in the  $T$  dependence[35]. Our films all exhibit a broadened kink around  $T^*$ , shown in Fig. 3(c). The change in temperature of this feature was very small, approximately 12K lower for the tensile strained samples, similar to the changes reported for external pressure[35]. For the tensily strained samples a lower value of 190K was found, possibly due to the thin film

nature of the films[53]. For LAO, with very small compressive strain, the value is shifted upward to 203 K. For SLAO the value is shifted to 207 K, strongly suggesting the Neel temperature for these films is shifted higher with higher strain, analogous to the effect of external pressure found by Zhou *et al.*, however a different mechanism must be responsible, as  $\Delta$  is not constant, discussed below. Resonant x-ray scattering measurements are needed in order to further confirm these changes in  $T_N$  and investigate any possible changes in magnetic structure, which cannot be investigated via transport.

XAS is an excellent experimental tool to study electronic structure which has been extensively utilized in the study of  $\text{ReNiO}_3$  perovskites[12, 54, 55]. Though TEY mode is a surface sensitive tool, the smaller thickness ( $\sim 6 \text{ nm}$ ) of these films compared to probing depth ( $\sim 12 \text{ nm}$ ) of TEY mode allowed us to explore the electronic structure of the entire film. The strong white line at 855 eV (872eV) corresponds to the  $L_3$  ( $L_2$ ) edge transition from the  $d^7$ :  $t_{2g}^6 e_g^1$  ground state to the  $ct_{2g}^6 e_g^2$  ( $c$  denotes a core hole) excited state. Another lower energy peak,  $\sim 853 \text{ eV}$ , which corresponds to the same electronic transition, is due to a multiplet interaction between the core hole and the excited electron when strong localization is present, becoming prominent for the highly tensile strained samples. This systematic change in the multiplet /  $L_3$  relative position and intensity holds valuable information about the hybridization of the  $d^7$  and  $d^8\bar{L}$  states. The quantitative value of the observed splitting, which is found to be related with the CT energy ( $\Delta$ ) has been plotted in Fig. 4(b)[52]. As can be seen, this splitting begins decreasing as the films are further compressed in the  $a$ - $b$  plane, indicating a change in the covalence between Ni and O is likely causing the observed transport properties. To confirm this explanation cluster calculations were carried out using  $\Delta$  as a control parameter, Fig. 4(b) (right side). As shown changing  $\Delta$  reproduces the observed splitting, with a corresponding value of  $\sim 2.5 \text{ eV}$  (for the tensile strained samples) and being reduced down to  $\sim 0.65 \text{ eV}$  in the case of YAO.

The large reduction in  $\Delta$  (approximately 1/4th of the saturated value for ENO on YAO) implies the covalence is strongly increased between Ni- $d$  and O- $p$  orbitals. This can be understood in terms of changes in the Ni-O-Ni bond; as the lattice is compressed in plane an increase in the overlap of the O:  $p_{x,y}$  and Ni:  $d_{x^2-y^2}$  orbitals occurs. The increasing covalence is strongly reminiscent of what was seen for A-site cation exchange (Fig. 1)[26]. For the tensilely strained samples, using similar analysis, the overlap would decrease, leading to a reduction in covalence, however the splitting appears to remain unchanged with increasing tensile strain. These results indicate that as the strain is changed from compressive to tensile the  $d^8\bar{L}$  state is effectively decoupled from the  $d^7$  state. Park *et al* have recently proposed, using DFT + DMFT, a site-selective Mott state, where the insulating gap is determined by the singlet formation energy between an O- $p$  hole and Ni- $d$  electron[33], our results are compatible with their predictions, showing the decoupling of the  $d^7$  and the  $d^8\bar{L}$  states leads to an insulating state. Further corroborating our results, Wang *et al* recently showed that the insulating regime is largely controlled by the number of  $d$  electrons, not the intraelectronic

repulsion, which is strongly dependent on the charge transfer from oxygen atoms[58]. To further investigate this effect and confirm our conclusions, resonant x-ray scattering measurements will be performed to investigate the evolution of the bond lengths and angles with strain.

## V. CONCLUSION

To summarize, epitaxial ultrathin films of ENO grown on a variety of substrates spanning both compressive and tensile strain were investigated with XRD, electronic transport, XAS, and cluster calculations. The sample's properties were found to be highly tunable with strain, shifting the MIT tantalizingly close to room temperature and only effecting  $T_N$  to a small extent. These results indicate the transitions remains second-

order, showing a key difference between epitaxial strain and A-site exchange or doping and implying the application of compressive strain mimics external pressure. Through XAS and cluster calculations it was determined that compressive strain enhances the covalence of the Ni-d and O-p orbitals, leading to an entirely metallic state. These results showcase ENO's potential utility for future device applications, as the MIT can be shifted from the high bulk value of 480K to near room temperature or to being entirely quenched without the complication of using different materials or chemical doping.

JC was funded by grants from majority DOD-ARO (W911NF-11-1-0200) and partially NSF (DMR-0747808). Work at the Advanced Photon Source is supported by the U.S. Department of Energy, Office of Science under grant No. DEAC02-06CH11357.

- 
- [1] Masatoshi Imada, Atsushi Fujimori, and Yoshinori Tokura, *Rev. Mod. Phys.* **70**, 4 (1998).
  - [2] J. Chakhalian, J. W. Freeland, H.-U. Habermeier, G. Cristiani, G. Khaliullin, M. van Veenendaal, and B. Keimer, *Science* **318**, 1114 (2007).
  - [3] J. Chakhalian, J. W. Freeland, G. Sprajer, J. Strempler, G. Khaliullin, J. C. Cezar, T. Charlton, R. Dalgliesh, C. Bernhard, G. Cristiani, H.-U. Habermeier, and B. Keimer, *Nature Physics* **2**, 244 (2006).
  - [4] Y. Tokura, *Rep. Prog. Phys.* **69**, 797 (2006).
  - [5] M. McCormack, S. Jin, T. H. Tiesel, R. M. Fleming, and Julia M. Phillips, *Appl. Phys. Lett.* **64**, 22 (1994).
  - [6] J. Wang, J. B. Neaton, H. Zheng, V. Nagarajan, S. B. Ogale, B. Liu, D. Viehland, V. Vaithyanathan, D. G. Schlom, U. V. Waghmare, N. A. Spaldin, K. M. Rabe, M. Wuttig, and R. Ramesh, *Science* **299**, 1719 (2003).
  - [7] V. Laukhin, J. Fontcuberta, J. L. Garca-Muoz, and X. Obradors, *Phys. Rev. B* **56**, R10009 (1997).
  - [8] H. Kuwahara, Y. Tomioka, A. Asamitsu, Y. Moritomo, and Y. Tokura, *Science* **270**, 961 (1995).
  - [9] Jian Liu, M. Kareev, D. Meyers, B. Gray, P. Ryan, J. W. Freeland, and J. Chakhalian, *Phys. Rev. Lett.* **109**, 107402 (2012).
  - [10] K. Ghosh, S. B. Ogale, R. Ramesh, R. L. Greene, T. Venkatesan, K. M. Gapchup, R. Bathe, and S. I. Patil, *Phys. Rev. B* **59**, 533 (1999).
  - [11] C. H. Ahn, J.-M. Triscone, and J. Mannhart, *Nature* **424**, 1015 (2003).
  - [12] Jian Liu, M. Kareev, B. Gray, J. W. Kim, P. Ryan, B. Dabrowski, J. W. Freeland, and J. Chakhalian, *Appl. Phys. Lett.* **96**, 233110 (2010).
  - [13] Ashutosh Tiwari, C. Jin, and J. Narayan, *Appl. Phys. Lett.* **80**, 21 (2002).
  - [14] Zuhuang Chen, Xi Zou, Wei Ren, Lu You, Chuanwei Huang, Yurong Yang, Ping Yang, Junling Wang, Thirumany Sritharan, L. Bellaiche, and Lang Chen, *Phys. Rev. B* **86**, 235125 (2012).
  - [15] S. El Helali, K. Daoudi, A. Fouzri, M. Oumezzine, M. Oueslati, and T. Tsuchiya, *Appl. Phys. A* **108**, 379 (2012).
  - [16] A. Biswas, M. Rajeswari, R. C. Srivastava, T. Venkatesan, R. L. Greene, Q. Lu, A. L. de Lozanne, and A. J. Millis, *Phys. Rev. B* **63**, 184424 (2001).
  - [17] J. Zhang, H. Tanaka, T. Kanki, J.-H. Choi, and T. Kawai, *Phys. Rev. B* **64**, 184404 (2001).
  - [18] X. J. Chen, S. Soltan, H. Zhang, and H.-U. Habermeier, *Phys. Rev. B* **65**, 174402 (2002).
  - [19] A. T. Zayak, X. Huang, J. B. Neaton, and Karin M. Rabe, *Phys. Rev. B* **74**, 094104 (2006).
  - [20] D. Fuchs, C. Pinta, T. Schwarz, P. Schweiss, P. Nagel, S. Schuppler, R. Schneider, M. Merz, G. Roth, and H. v. Lhneysen, *Phys. Rev. B* **75**, 144402 (2007).
  - [21] D. Fuchs, E. Arac, C. Pinta, S. Schuppler, R. Schneider, and H. v. Lhneysen, *Phys. Rev. B* **77**, 014434 (2008).
  - [22] A. D. Rata, A. Herklotz, K. Nenkov, L. Schultz, and K. Drr, *Phys. Rev. Lett.* **100**, 076401 (2008).
  - [23] H.W. Jang, S. H. Baek, D. Ortiz, C. M. Folkman, R. R. Das, Y. H. Chu, P. Shafer, J. X. Zhang, S. Choudhury, V. Vaithyanathan, Y. B. Chen, D. A. Felker, M. D. Biegalski, M. S. Rzchowski, X. Q. Pan, D. G. Schlom, L. Q. Chen, R. Ramesh, and C. B. Eom, *Phys. Rev. Lett.*, **101**, 107602 (2008).
  - [24] J. H. Lee and K. M. Rabe, *Phys. Rev. Lett.* **104**, 207204 (2010).
  - [25] J. H. Lee, L. Fang, E. Vlahos, X. Ke, Y. W. Jung, L. F. Kourkoutis, J.-W. Kim, P. J. Ryan, T. Heeg, M. Roeckerath, V. Goian, M. Bernhagen, R. Uecker, P. C. Hammel, K. M. Rabe, S. Kamba, J. Schubert, J. W. Freeland, D. A. Muller, C. J. Fennie, P. Schiffer, V. Gopalan, E. Johnston-Halperin and D. G. Schlom, *Nature (London)* **466**, 954 (2010).
  - [26] María Luisa Medarde, *J. Phys.: Condens. Matter* **9**, 1679 (1997).
  - [27] J. B. Torrance, P. Lacorre, A. I. Nazzari, E. J. Ansaldo, and Ch. Niedermayer, *Phys. Rev. B* **45**, 14 (1992).
  - [28] M. K. Stewart, Jian Liu, R. K. Smith, B. C. Chapler, C.-H. Yee, D. Meyers, R. E. Baumbach, M. B. Maple, K. Haule, J. Chakhalian, and D. N. Basov, *J. Appl. Phys.* **110**, 033514 (2011).
  - [29] A. Caytuelo, H. Micklitz, M. M. Abd-Eleguid, F. J. Litterst, J. A. Alonso, and E. M. Baggio-Saitovich, *Phys. Rev. B* **76**, 193105 (2007).
  - [30] J. E. Lorenzo, J. L. Hodeau, L. Paolasini, S. Lefloch, and G. Demazeau, *Phys. Rev. B* **71**, 045128 (2005).
  - [31] V. Scagnoli, U. Staub, M. Janousch, A. M. Mulders, and M. Shi, *Phys. Rev. B* **72**, 155111 (2005).
  - [32] Y. Bodenthin, U. Staub, C. Piamonteze, M. García-Fernández, M. J. Martínez-Lope, and J. A. Alonso, *J. Phys.: Condens. Matter* **23**, 036002 (2011).
  - [33] Hyowon Park, Andrew J. Millis, and Chris A. Marianetti, *Phys.*



- Rev. Lett. **109**, 156402 (2012).
- [34] C. Piamonteze, H. C. N. Tolentino, A. Y. Ramos, N. E. Massa, J. A. Alonso, M. J. Martínez-Lope, and M. T. Casais, *Physica B* **320**, 71 (2002).
  - [35] J.-S. Zhou, J. B. Goodenough, and B. Dabrowski, *Phys. Rev. Lett.* **95**, 127204 (2005).
  - [36] G. Frand, O. Bohnke, P. Lacorre, and J. L. Forquet, *Journal Solid State Chem.* **120**, 157 (1995).
  - [37] Jiří Chaloupka and Giniyat Khaliullin, *Phys. Rev. Lett.* **100**, 016404 (2008).
  - [38] W. L. Lim, E. J. Moon, J. W. Freeland, D. J. Meyers, M. Kareev, J. Chakhalian, and S. Urazhdin, *Appl. Phys. Lett.* **101**, 143111 (2012).
  - [39] S. Asanuma, P.-H. Xiang, H. Yamada, H. Sato, I. H. Inoue, H. Akoh, A. Sawa, K. Ueno, H. Shimotani, H. Yuan, M. Kawasaki, and Y. Iwasa, *Appl. Phys. Lett.* **97**, 142110 (2010).
  - [40] Raoul Scherwitzl, Pavlo Zubko, I. Gutierrez Lezama, Shimpei Ono, Alberto F. Morpurgo, Gustau Catalan, and Jean-Marc Triscone, *Adv. Mater.* **22**, 5517 (2010).
  - [41] P. Lacorre, J. B. Torrance, J. Pannetier, A. I. Nazzal, P. W. Wang, and T. C. Huang, *Journal Solid State Chem.* **91**, 225 (1991).
  - [42] M. J. Martínez-Lope and J. A. Alonso, *Eur. J. Solid-State Inorg. Chem.* **32**, 361 (1995).
  - [43] S. Middey, D. Meyers, M. Kareev, E. J. Moon, B. A. Gray, X. Liu, J. W. Freeland, and J. Chakhalian, *Appl. Phys. Lett.* **101**, 261602 (2012).
  - [44] D. Meyers, E. J. Moon, M. Kareev, I. C. Tung, B. A. Gray, Jian Liu, M. J. Bedzyk, J. W. Freeland, and J. Chakhalian, *arXiv:1112.5348*
  - [45] J.-G. Cheng, J.-S. Zhou, J. B. Goodenough, J. A. Alonso, and M. J. Martínez-Lope, *Phys. Rev. B* **82**, 085107 (2010).
  - [46] R. Lengsdorf, A. Barla, J. A. Alonso, M. J. Martínez-Lope, H. Micklitz, and M. M. Abd-Elmeguid, *J. Phys.: Condens. Matter* **16**, 3355 (2004).
  - [47] I. I. Mazin, D. I. Khomskii, R. Lengsdorf, J. A. Alonso, W. G. Marshall, R. M. Ibberson, A. Podlesnyak, M. J. Martínez-Lope, and M. M. Abd-Elmeguid, *Phys. Rev. Lett.* **98**, 176406 (2007).
  - [48] R. D. Sánchez, M. T. Causa, A. Seoane, J. Rivas, F. Rivadulla, M. A. López-Quintela, J. J. Pérez Cacho, J. Blasco, and J. García, *Journal of Solid State Chem.* **151**, 1 (2000).
  - [49] M. A. van Veenendaal and G. A. Sawatzky, *Phys. Rev. B* **50**, 11326 (1994).
  - [50] J. Chakhalian, J. M. Rondinelli, Jian Liu, B. A. Gray, M. Kareev, E. J. Moon, N. Prasai, J. L. Cohn, M. Varela, I. C. Tung, M. J. Bedzyk, S. G. Altendorf, F. Strigari, B. Dabrowski, L. H. Tjeng, P. J. Ryan, and J. W. Freeland, *Phys. Rev. Lett.* **107**, 116805 (2011).
  - [51] F. Rivadulla, J.-S. Zhou, and J. B. Goodenough, *Phys. Rev. B* **67**, 165110 (2003).
  - [52] Jian Liu, S. Okamoto, M. van Veenendaal, M. Kareev, B. Gray, P. Ryan, J. W. Freeland, and J. Chakhalian, *Phys. Rev. B* **83**, 161102(R) (2011).
  - [53] M. Ziese, H. C. Semmelhack, and K. H. Khan, *J. Appl. Phys.* **91**, 12 (2002).
  - [54] Masaichiro, Naoki Ishimatsu, Naomi Kawamura, Masaki Azuma, Yuichi Shimakawa, Mikio Takano, and Takayuki Uozumi, *Phys. Rev. B* **80**, 233104 (2009).
  - [55] M. Medarde, A. Fontaine, J. L. García-Muñoz, J. Rodríguez-Carvajal, M. de Santis, M. Sacchi, G. Rossi, and P. Lacorre, *Phys. Rev. B* **46**, 23 (1992).
  - [56] T. J. Regan, H. Ohldag, C. Stamm, F. Nolting, J. Lüning, J. Stöhr, and R. L. White, *Phys. Rev. B* **64**, 214422 (2001).
  - [57] J. Zaanen, G. A. Sawatzky, and J. W. Allen, *Physical Review Letters* **55**, 4 (1985).
  - [58] Xin Wang, M. J. Han, Luca de' Medici, Hyowon Park, C. A. Marianetti, and Andrew J. Millis, *Phys. Rev. B* **86**, 195136 (2012).

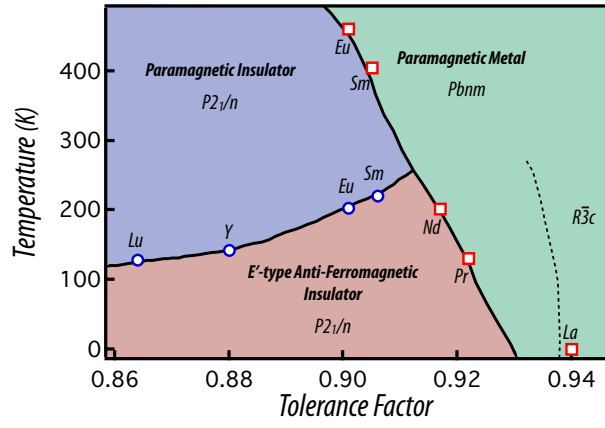


FIG. 1: (Color online) Phase diagram for the nickelates of different A-sites, data taken from Lengsdorg *et al*[46]

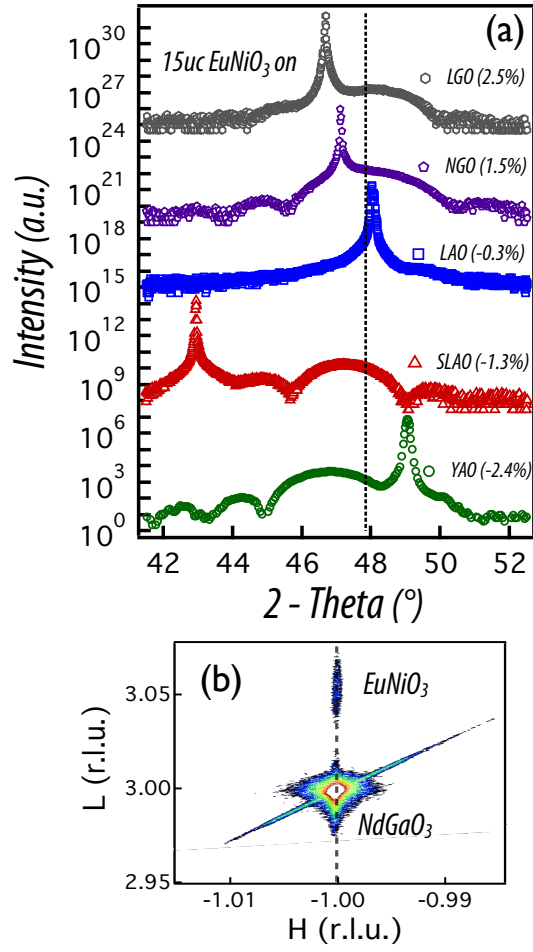


FIG. 2: (Color online) (a) XRD data for 15uc ENO samples on various substrates. The shifting from the bulk lattice value (indicated by the dashed line) is apparent for the compressively strained samples. (b) RSM for a 35uc ENO film grown on NGO showing the film is coherently strained.

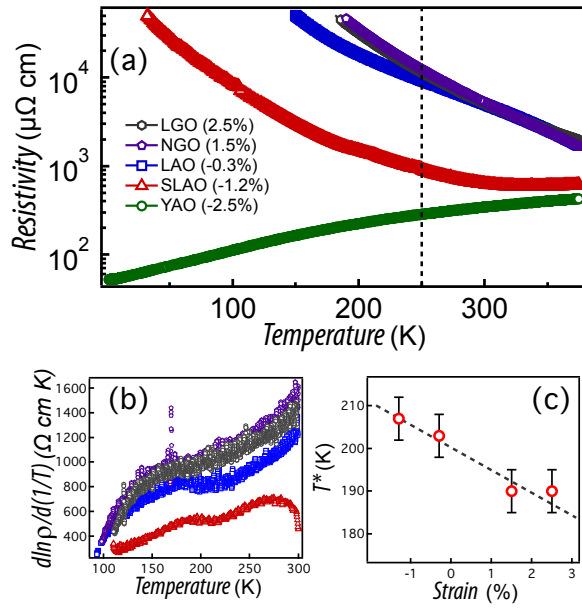


FIG. 3: (Color online) (a) Transport data for 15uc ENO samples on various substrates. The dashed line indicates the temperature where the XAS data was taken (Fig. 4a). (b)  $d\ln(\rho)/d(1/T)$  data for the films. (c)  $T^*$  for various strains.



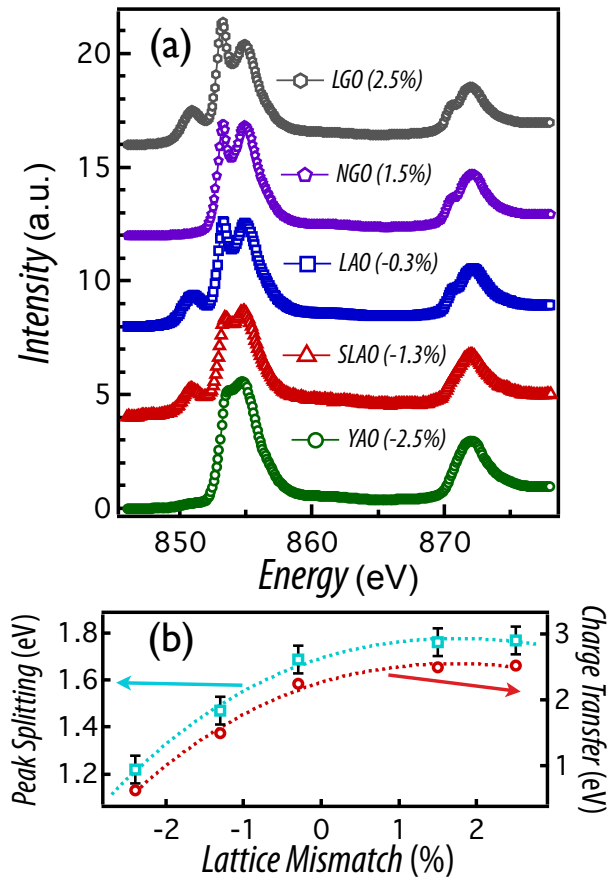


FIG. 4: (Color Online) (a) XAS data for 15uc ENO samples on various substrates showing the change in the pre edge peak with strain. (b) The experimentally obtained peak splitting along with the theoretically obtained corresponding CT energy.